J. Phys.: Condens. Matter 7 (1995) 10059–10073. Printed in the UK

A spectroscopic study of the structure of amorphous hydrogenated carbon

J K Walters†, R J Newport†, S F Parker‡ and W S Howells‡

† Physics Laboratory, The University, Canterbury, Kent CT2 7NR, UK
‡ Rutherford Appleton Laboratory, Didcot, Oxon OX11 0QX, UK

Received 14 August 1995, in final form 27 October 1995

Abstract. A range of amorphous hydrogenated carbon (a-C:H) samples have been studied using inelastic neutron spectroscopy (INS) and Fourier transform infrared (FTIR) spectroscopy. Using these complementary techniques, the bonding environments of both carbon and hydrogen can be probed in some detail, with the INS data providing not only qualitative but also quantitative information. By comparing the data from each of the samples we have been able to examine the effects of different deposition conditions, i.e. precursor gas, deposition energy and deposition method, on the atomic-scale structure of a-C:H.

1. Introduction

The importance of amorphous hydrogenated carbon (a-C:H) as a novel coating material has already been established in terms of both its actual and potential applications [1, 2]. In general, the most commonly exploited properties of a-C:H are its hardness, resistance to chemical attack, histocompatibility and transparency to infrared. However, the properties of this material are critically dependent on the conditions under which it was deposited [3], and the precise nature of this relationship is not well understood. a-C:H can be produced in a variety of forms, ranging from the extremes of soft polymeric (high hydrogen content and high sp^3 content with many $-CH_2-$ chains) and graphitic (low hydrogen content and high sp^2 content) forms, to hard or 'diamond-like' a-C:H which has mixed bonding and a large degree of structural rigidity and cross-linking. It is therefore of crucial importance to find a model whereby the relationship between the macroscopic properties of the material and the deposition conditions can be understood. Once this has been achieved, the possibility of producing tailor-made a-C:H coatings becomes viable.

In spite of the great potential of the material and the studies so far undertaken, e.g. [3, 4, 5], the structure of these materials at the atomic level is not fully understood; this is of course largely due to the range of potential bonding environments which allows complex mixing of atomic-scale correlations. However, it is self-evident that the bonding in a-C:H has a vital role in determining the observed properties; of particular importance will be the proportions of sp^2 and sp^3 carbon bonding environments. Perhaps the most widely accepted current model for the atomic structure of a-C:H is that developed by Robertson [6, 3, 7]. Here clusters of sp^2 carbon are linked via a hydrogenated (or polymeric) sp^3 phase, where it is proposed that the mechanical properties are governed by these interconnections, and the sp^2 regions determine the electronic properties. Within this model, hydrogen is seen to stabilize the sp^3 regions, reducing the size of any sp^2 clusters, but at the same time

0953-8984/95/5010059+15$19.50

increasing the number of network-terminating bonds, leading to a maximum hardness at intermediate hydrogen concentrations [8]. A fuller account of this model can be found in reviews by Angus [8] and Robertson [3].

Our own neutron diffraction data [9], together with other experimental [10, 11] and molecular dynamics simulation work [12] has, however, provided clear evidence of the inadequacies of this model, and has formed the basis for an improved model structure [13]. Essentially this consists of short sections (<5 carbon atoms) of sp^3 CH_2 chains, and statistically distributed CH groups in an sp^2–sp^3 carbon network with olefinic rather than graphitic carbons. These two environments are separated by regions of non-hydrogenated sp^2 carbons. Neutron diffraction data [14, 9] have also provided evidence for the presence of molecular hydrogen in some way 'trapped' within the amorphous network. It is in the context of this model that the present experimental data are discussed.

Building on our work on annealing a-C:H [15], this paper presents the results of inelastic neutron scattering (INS) and infrared (IR) spectroscopy experiments performed on a range of a-C:H samples, which will be used to provide additional insight into the carbon and hydrogen bonding environments present in a-C:H, with reference to our revised model structure, and to examine the effects of deposition parameters.

The effective deposition energy is already known to be a crucial parameter in determining the properties and overall structural nature of the deposited film [16, 17, 18]. Also, the effective impact energy at the growth volume is dependent on the spectrum of fragment sizes derived from the source, and therefore on the nature of the precursor gas, and of course on the physical processes involved in the ionization/decomposition processes associated with the method of deposition. The basis of models currently used to relate deposition parameters to the structure of the deposited material is the 'subplantation' model of Lifshitz and co-workers [19] (and this is expounded in the a-C:H context by Robertson [3]). Generally, for deposition from a hydrocarbon species, polymer hydrocarbon film formation occurs at low growth impact energies (~10 s of eV), amorphous hydrogenated carbon films form at intermediate impact energies (~50–100 eV), and dense, diamond-like carbon (with a relatively low hydrogen content) is formed at high energies (~100–200 eV). For impact energies higher than ~500 eV, disordered graphitic films are expected to result (due to the large amount of damage caused by impinging species) with a low sp^3 carbon content. These spectroscopic data will complement the neutron diffraction studies already undertaken [20].

IR spectroscopy is a widely used technique in the study of these materials—see, e.g. [21, 22, 23]—especially for investigating the hydrogen bonding environment. Previously, Dischler [21] performed an extensive study of the bonding of hydrogen in a-C:H, and proposed assignments for all the observed frequencies. Also, Vandentrop *et al* [23] used IR spectroscopy to estimate CH_2:CH_3 ratios, but all IR results necessarily depend upon assumptions for the matrix elements of each vibration, making fully quantitative analysis very difficult. The technique has, however, been used quite successfully to look at trends among different samples [15, 24]. This kind of information can be extremely useful and is how the IR data have been used in this paper.

INS does not suffer from this problem as the observed scattering intensity is directly related to the eigenvector of the vibration, although the energy resolution is not as good as for IR spectra. In addition, there are no forbidden transitions in the INS case. INS data are most useful for looking at the region of low-energy vibrations (~400–1800 cm^{-1}, i.e. ~50–225 meV)—that is, CH_2 and CH_3 deformations and carbon–carbon stretches. As well as for the a-C:H samples, spectra for diamond and graphite powders, polyethylene and polyisoprene (natural rubber) have also been recorded and provide 'reference' spectra

against which those for a-C:H can be compared. The TFXA spectrometer at the ISIS pulsed neutron source (Rutherford Appleton Laboratory, UK) is well suited to determining the vibrational density of states of hydrogenated materials as it is optimized for energy resolution ($\Delta E/E \sim 1.5$–3%), albeit with a resultant loss in Q-resolution [25].

So, a combination of these two spectroscopic methods, IR (frequencies and relative peak intensities) and INS (low frequencies and peak intensities), enables the relative proportions and assignments of different bonding environments to be determined with a higher degree of reliability.

2. Experimental details and data analysis

2.1. Sample preparation

The preparation conditions and properties of each of the samples studied are summarized in table 1, and more information can be found in [9, 26, 27, 28]. For the samples prepared using the fast-atom-beam source (FAB) the energy given is the effective source energy and the sample densities were determined using a residual volume method. For the samples prepared by plasma-enhanced chemical vapour deposition (PECVD) the energy values given are mean ion energies for particles in the beam and the densities were determined by a flotation method. The hydrogen content of all the samples was obtained by combustion analysis and the ratios of carbon bond types are from the results of neutron diffraction experiments [19, 20].

Table 1. Information on sample deposition and properties.

Sample	Method of deposition	Precursor gas	Beam energy (eV)	Density (g cm^{-3})	H content (at.%)	sp^1:sp^2:sp^3 CC bonds†	Knoop hardness (kg mm^{-2})
I	FAB	C_2H_2	~500	1.8	35	0:0.4:1	~2000 [37]
II	FAB	C_3H_8	~500	2.0	32	0:0.4:1	~2000 [37]
III	FAB	C_2H_2	~800	1.2	22	0.05:0.3:1	Unknown
IV	FAB	C_6H_{12}	~960	1.5	25	0.04:0.46:1	Unknown
V	PECVD	C_2H_2	~30	1.6	45	0.13:0.14:1	500 [26]
VI	PECVD	C_2H_2	125	1.7	34	0.14:0:1	1200 [26]
Diamond	—	—	—	3.51	0	0:0:1	10 000 [38]
Graphite	—	—	—	2.26	0	0:1:0	— [39]
Polyethylene	—	—	—	0.93	66	0:0:1	— [40]
Rubber	—	—	—	0.96	60	0:0.25:1	—

† Obtained from neutron diffraction data.

2.2. Infrared spectroscopy

IR measurements were performed using a Fourier transform infrared spectrometer (model Bio Rad FTS60). Almost all of these a-C:H samples have a high reflectivity, so it was necessary to take two different kinds of measurement for the high- and low-energy regions of the spectrum. For the carbon–carbon stretches and CH_n deformations (low energy), the best quality data was obtained from diffuse reflectance measurements. However, for the CH stretch region (high-energy), photo-acoustic measurements gave better quality spectra.

Given the intrinsic difficulties associated with any attempt to analyse IR data quantitatively, we here concentrate on using Gaussian peak fits to the fundamental CH stretch

modes to examine the overall nature of the hydrogen bonding environment and its variation between the different samples. In the low-energy region broad vibrational assignments to the observed frequencies are given, but primarily it is the trends with changing deposition parameters which are examined. In this region, the assignment of observed frequencies is assisted by comparison with 'reference' spectra for diamond and graphite powders.

2.3. Inelastic neutron scattering

The INS data were collected on the TFXA spectrometer at the ISIS spallation neutron source, Rutherford Appleton Laboratory (UK) [25]. This spectrometer is used to collect the H-dominated incoherent INS data, where it generates high-intensity data integrated over momentum transfer. In the incoherent approximation [29], the scattering function can be directly related to the vibrational density of states, $g(\omega)$:

$$S^s(Q,\omega) = \frac{\hbar Q^2}{2m} e^{-2W} \frac{(1+\langle n_\lambda \rangle)}{\omega} g(\omega) \tag{1}$$

where $S^s(Q,\omega)$ is the self-scattering, $\hbar Q$ is the momentum transfer, $\hbar\omega$ the energy transfer, $\langle n_\lambda \rangle$ is the population factor for a mode of frequency ω_λ, and e^{-2W} is the Debye–Waller factor. A more complete account of the theory is given elsewhere [29, 30]. It should be noted that in an amorphous system such as a-C:H, there is a range of possible bonding environments which gives rise to vibrations over a spread of frequencies.

Table 2. Frequency assignments and areas obtained from the Gaussian fitting of CH stretch region of the IR data. (Note that where more than one Gaussian peak lies within the observed frequency range the total area of the peaks is given.)

Vibration	sp^2CH (olefinic/aromatic)	sp^3CH_3 (asymmetric)	sp^3CH_2 (asymmetric) and sp^3CH	sp^3CH_2 and sp^3CH_3 (symmetric)
Observed frequency	3035–2971	2977–2958	2930–2915	2870–2858
Sample I	1.75	4.55	14.35	14.35
Sample II	7.04	4.48	12.16	12.48
Sample III	1.32	2.2	12.1	6.16
Sample IV	2.0	1.25	16.0	10.25
Sample V	3.52	3.08	26.4	11.0
Sample VI	11.9	11.9	13.6	8.5

Unlike in previous experiments on a-C:H [31, 32], these samples were not quenched in liquid nitrogen before insertion into the cryostat (a procedure which in the past led to the low-energy-transfer region of the spectra being dominated by nitrogen modes) and this enables one to observe modes only associated with carbon and hydrogen bonding environments.

3. Results and discussion

In a detailed examination of the spectroscopic results it is more instructive to consider the two different regions of the spectra, 3400–2600 cm^{-1} (the CH stretch region) and 1800–10 cm^{-1} (the CC stretch and CH_n deformation region), separately to begin with; we will then attempt to correlate the findings from both in a summary. Figures 1 and 2, then, show the complete IR and INS spectra, respectively, for each of the a-C:H samples.

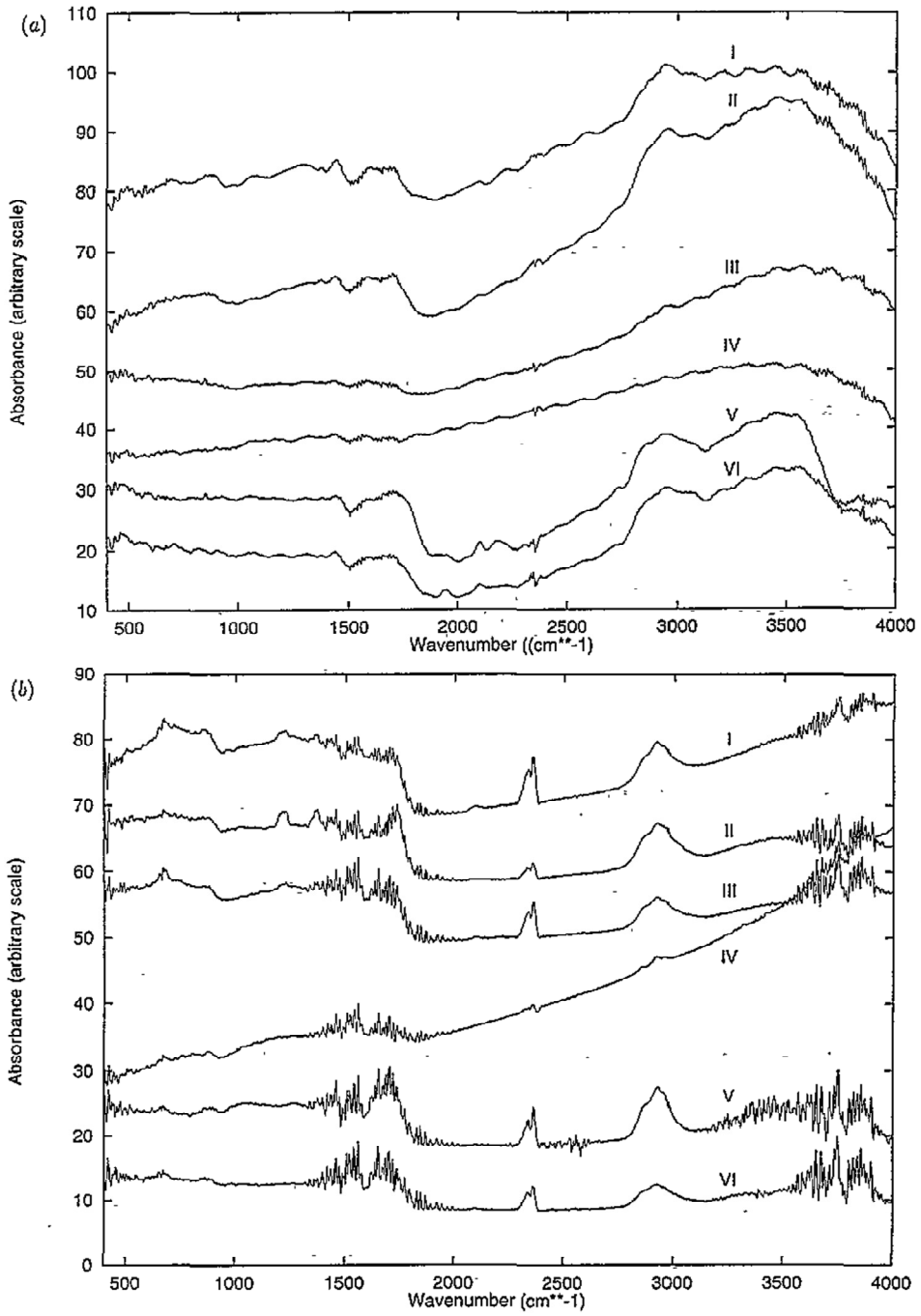

Figure 1. (a) Diffuse reflectance FTIR spectra for the a-C:H samples (see table 1). (b) Photoacoustic IR spectra for the a-C:H samples (see table 1).

3.1. The CH stretch region: 3400–2600 cm^{-1}

Due to the poor resolution of the INS data in this region (300–500 meV), only IR data are discussed for the CH stretching modes. Following a 'background subtraction' using a

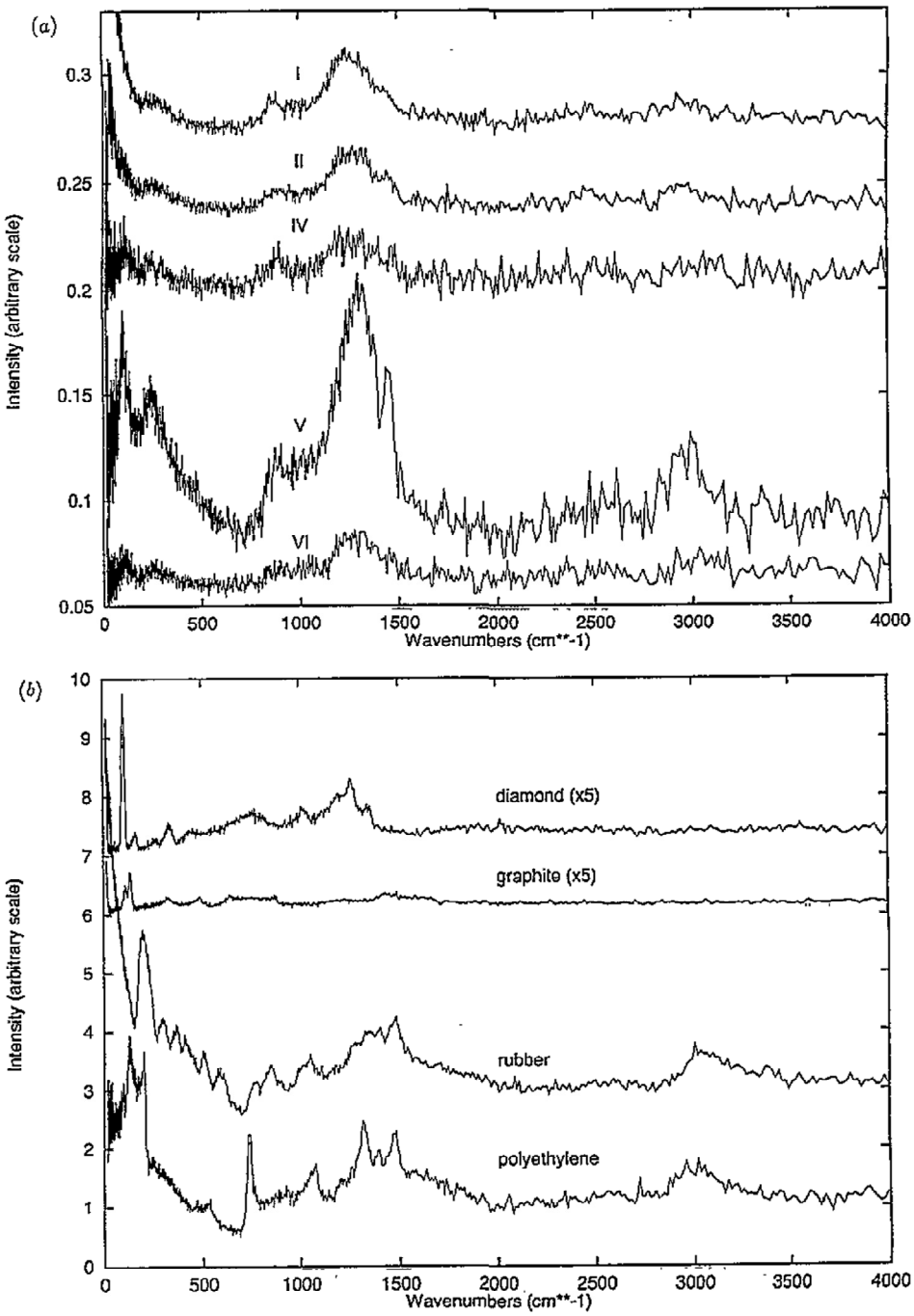

Figure 2. (a): Raw INS spectra for the a-C:H samples (see table 1). (b): Raw INS spectra for the 'standard' samples.

low-order polynomial, each spectrum is fitted with a series of Gaussians, allowing position and area to vary using the method of least squares until a best fit is found. Figure 3 shows the fitted Gaussians used to obtain a best fit for each sample. From the positions of the

Gaussians, assignment of the observed frequencies to vibrational modes can be made and the peak areas can be normalized to the hydrogen content of the sample and used to look at the relative proportions of each mode present in the samples. Table 2 gives the frequency and associated normalized peak areas derived from these data.

Now if we assume that the peaks associated with the anti-symmetric and symmetric stretching modes for the same group have the same area†, it is possible to determine the relative ratios, CH_2:CH_3, sp^3CH:sp^2CH and CH:CH_2, and these are shown in table 3. It is important to remember that these ratios are not absolute; comparisons are only meaningful in a relative way between samples.

Table 3. Approximate relative proportions of CH_n groups from the Gaussian fitting.

Sample	CH_2:CH_3	sp^3CH:sp^2CH	CH:CH_2
I	~2:1	~3:1	~1:1.2
II	~2:1	~1:1.5	~1.4:1
III	~2:1	~6:1	~2.4:1
IV	~7:1	~3.5:1	~1:1
V	~2:1	~6:1	~3:1

Before discussing these results in detail, it is worth pointing out that although frequencies associated with sp^2CH_2 and sp^2CH_3 groups are not observed (they are not clearly observed in IR spectra for a-C:H in general [33, 34, 35]), this is due to the weightings of their matrix elements and does not necessarily imply that these groups are absent. From figure 2 and table 2, it is clear that the four frequency assignments made are common to all of the samples. For sample VI the two high-frequency bands cannot be resolved, whereas for the other samples there are two peaks in this region (3035–2958 cm^{-1}). All samples do show that there is a mixture of sp^3CH and sp^2CH bonds and that both CH_2 and CH_3 groups are present, although the actual number of these cannot be determined. From figure 1(b) none of the samples show a peak at ~3300 cm^{-1} corresponding to sp^1CH, when it is known from neutron diffraction that two of the samples (III and VI) contain sp^1 carbon sites. This may simply be explained by the deterioration of the data quality which starts in this region of the spectra, as has been seen clearly in other IR studies [15].

Looking at table 3, the first thing to notice is that all the samples except one (IV) have approximately twice the peak area associated with CH_2 groups as with CH_3 groups: for sample IV, CH_2:CH_3 ~7:1. Since this ratio is the same for changes in deposition energy and method, and for preparation from propane and acetylene gases, it is reasonable to assume that this anomalous result is due to the use of cyclohexane (C_6H_{12}) as the precursor gas. This suggests that the relatively high deposition energy used is not sufficient to cause complete dissociation of the cyclohexane molecule, leaving fragments containing CH_2 groups which are incorporated into the a-C:H structure. The existence of such impacting fragments also means that the average energy per atom on impact is lower than if full dissociation had occurred. This could explain why CH_2 groups are not then broken up on impact. Evidence for some dissociation of the molecule is provided by the presence of CH_3 and CH groups. These impacting atoms and smaller fragments also cause etching of the growing film which is consistent with the observed CH:CH_2 ratio of areas of ~1:1, and with the measured hydrogen content of 25%.

† This assumption may not be valid; however, the conclusions drawn will be unaffected since only the differences between these ratios are discussed.

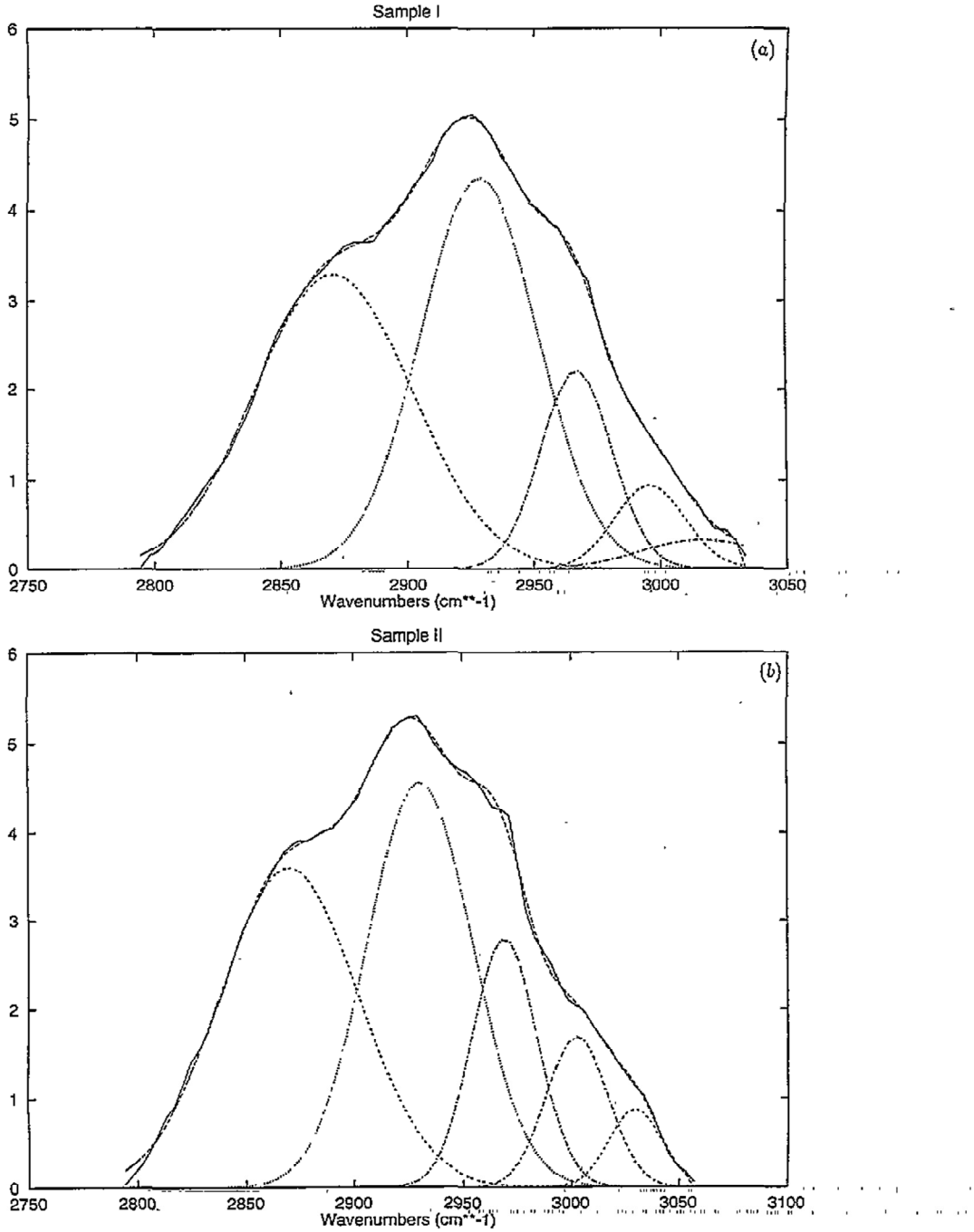

Figure 3. Gaussian fits obtained for the CH stretch region of the IR spectra showing constituent Gaussians for each a-C:H sample (see table 1).

Samples I and II, prepared from acetylene and propane, respectively, at the same deposition energy, show only slight differences and these are within the limits of experimental error. The presence of CH_2 groups indicates that these samples do have a

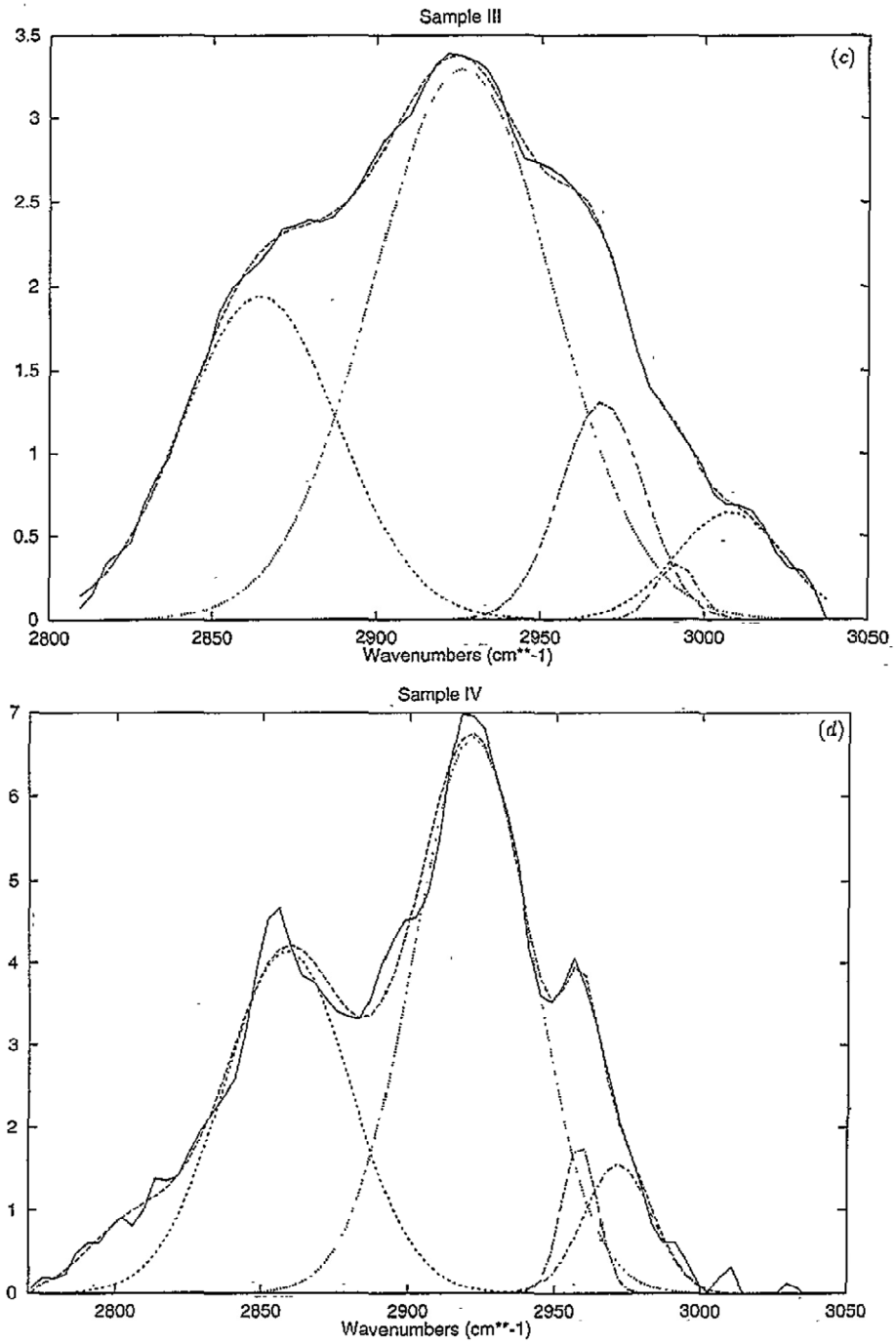

Figure 3. (Continued)

polymeric component, and the peak at ~2900 cm^{-1} (sp^2CH olefinic/aromatic) shows that olefinic/aromatic carbon–carbon bonds are present. This is all consistent with the results of neutron diffraction [9, 11] experiments on the same samples.

Now consider the effects of deposition energy for deposition using a fast-atom system

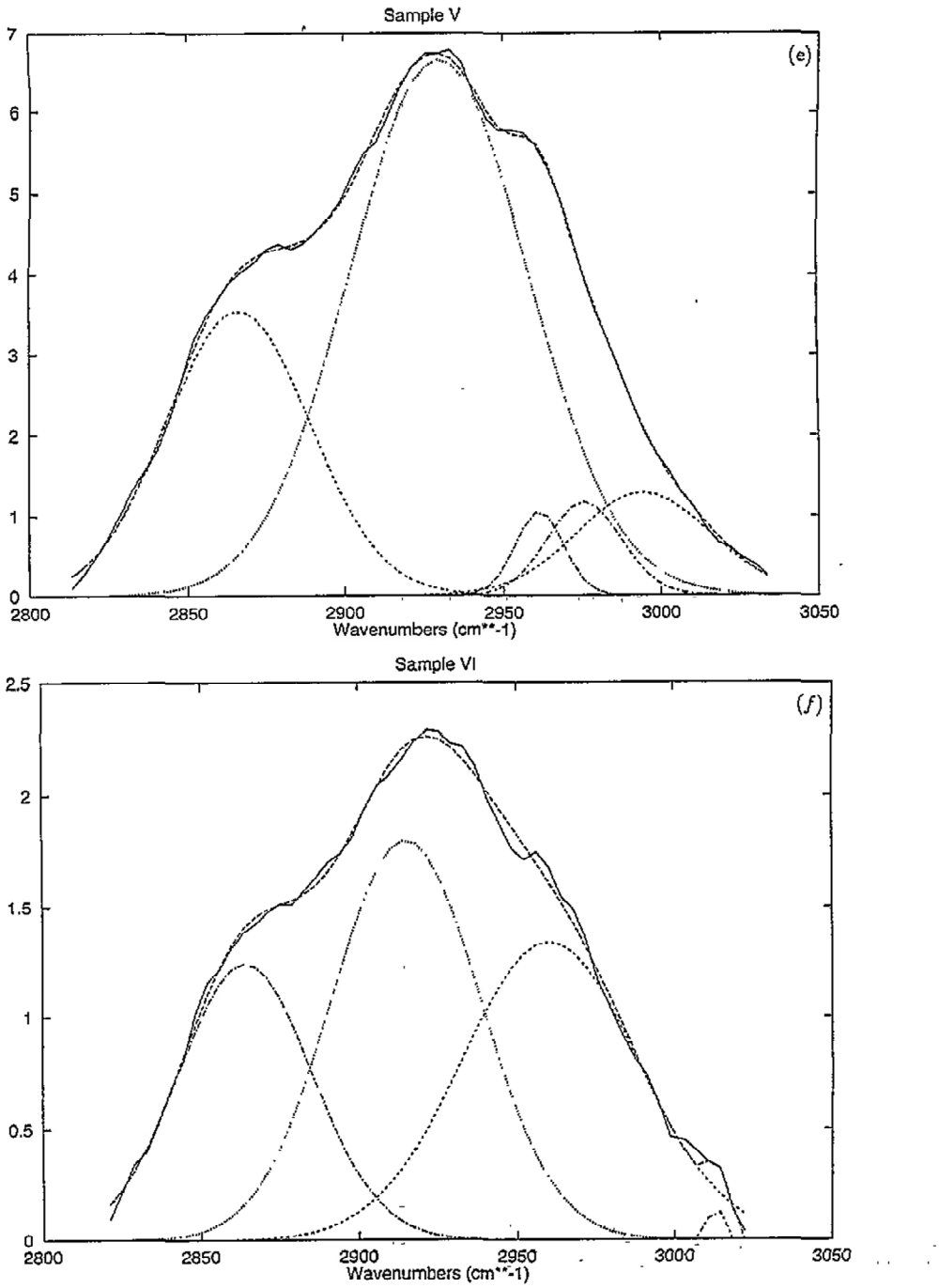

Figure 3. (Continued)

and acetylene gas, by looking at samples I and III. From the analysis of this CH stretch region, it is clear that the distribution of hydrogen within the network is quite different in each sample. Although a CH_2:CH_3 peak area ratio of ~2:1 is common to both samples, the sp^3CH:sp^2CH peak area ratios differ in that this is equal to ~3:1 for the lower-energy

sample (I) and ~6:1 for the higher-energy sample (III). The CH:CH_2 peak area ratios are also affected: ~1.2:1 for sample I and ~2.4:1 for sample III. From neutron diffraction experiments [20], it is known that in terms of the carbon network and the distribution of H–H, C–H and C–C bond lengths, these two samples are quite similar, although with this increase in energy it is found that there is a decrease in the number of sp^2 carbon bonds which, to some extent, could account for the relative increase in sp^3CH bonds. Also the increased peak area of CH relative to that of CH_2 groups for the higher-energy sample could be explained in terms of a more efficient etching of hydrogen for higher incident particle energies (i.e. within the subplantation model), but may also be a result of a more complete breaking up of the acetylene gas molecule at the higher energy—this could also account for the increased area associated with sp^3 carbon sites, in that there is an increased amount of energy to be dissipated on impact, which causes a larger thermal spike. The decreased relative number of CH_2 groups also means a decreased relative polymeric component in the higher-energy sample.

Finally, samples V and VI were both prepared by plasma-enhanced chemical vapour deposition (PECVD) from acetylene gas. Although resolution problems mean that the discussion is necessarily limited, it is clear that the distribution of hydrogen in sample V (low-energy PECVD) is very similar to that found in sample III (high-energy FAB), having a relatively low polymeric spectral component and relatively few CH_3 groups. Unfortunately, we are unable to make any further statements about these samples for this particular region of the spectrum.

3.2. The CC stretch and CH_n deformation region: 1800–10 cm^{-1}

For this region of the spectrum, INS experiments are the best source of structural information, although intensities at these low energy transfer values are difficult to interpret. The general assignments for this region are: 800–1000 cm^{-1} sp^2 C–H out-of-plane and in-plane bending; 1100–1300 cm^{-1} sp^3 C–C stretch and –CH_2 wag/twist; 1300–1500 cm^{-1} sp^3 CH_2 and CH_3 deformations; and 1500–1700 cm^{-1} sp^2 C=C and aromatic C=C stretches; intensity in the region 0–400 cm^{-1} is generally due to vibrations of large fragments of the lattice/network. The smoothed INS spectra shown in figure 4 show that these bands are common to all the a-C:H samples. However, improved insight into the structure of these materials can be gained if the data are compared to spectra for diamond, graphite and polyethylene powders, and polyisoprene (rubber) shown in figure 5. (Note that a similar, independent spectrum for polyethylene has already been published [36] showing that this spectrum is completely reproducible.)

In fact, this comparison produces some interesting results. The spectra for a-C:H are really quite dissimilar to those for diamond and graphite, but there is a much greater resemblance to the polymer spectra, with broadening of bands as is expected for an amorphous structure. In the first instance this is in agreement with the model for a-C:H described earlier [13]; however, the lack of a strong band at ~720 cm^{-1} due to CH_2 rocking in extended methylene chains (as seen in the polyethylene spectrum) is evidence that the CH_2 chains must be short and/or sparse, which is consistent with the results of neutron diffraction [9] and NMR [11] experiments. When making comparisons between the a-C:H samples and these standard materials, it is important to note that the high cross-section of hydrogen will mean that correlations involving hydrogen will tend to dominate the spectra, so it is impossible to say whether or not the carbon–carbon correlations are more similar to diamond or graphite.

Taking a more detailed look at the data, consider first the effect of the precursor gas by

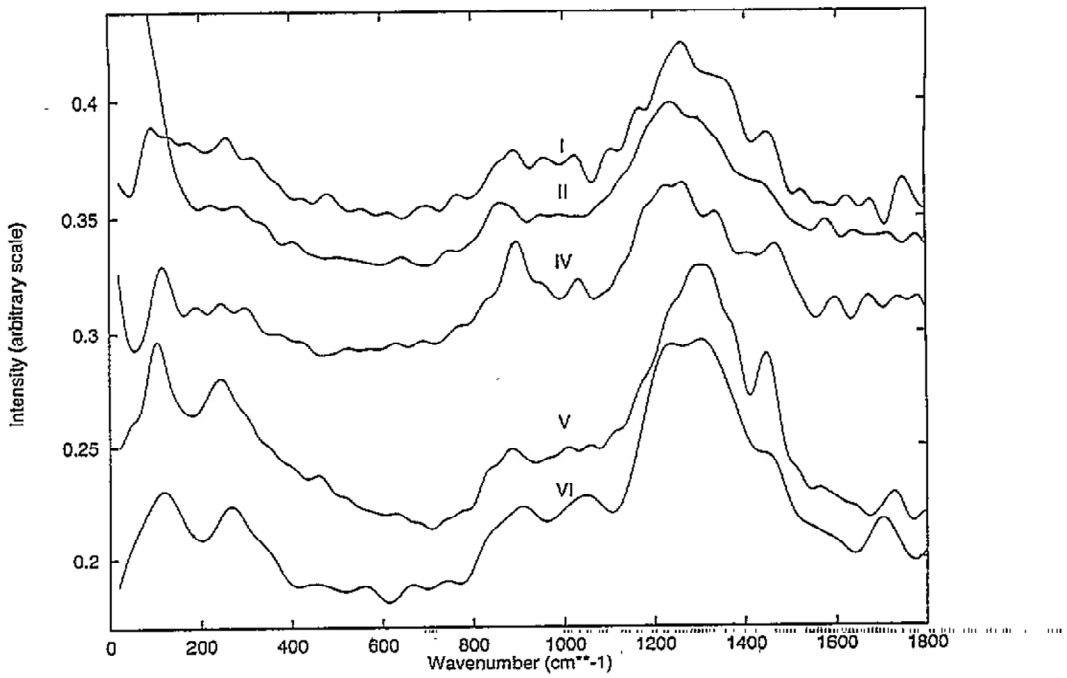

Figure 4. Smoothed INS data for the CC stretch and CH_n deformation region for the a-C:H samples (see table 1).

comparison of the spectra for samples I and II. The slightly higher sp^3 content of sample I is shown by the increased peak height at ~1250 cm^{-1}. The increased intensities of the peaks at 1300–1500 cm^{-1}, associated with deformations of C–H bonds, are also consistent with the higher hydrogen content of sample I, although the two samples have roughly the same proportion of sp^2 CH bonds (~850 cm^{-1}). Overall the spectra are very similar, as was the case for the CH stretch region, with both samples showing some evidence for the presence of sp^2 C=C stretch bands above 1500 cm^{-1}.

The spectra for sample IV, prepared from cyclohexane at a higher deposition energy, are quite different from those for samples I and II, although also more similar to those for the polymer samples than to the diamond and graphite powders. The strong peak at ~1250 cm^{-1} (sp^3 C–C stretch) is much weaker than in the previous two samples, whereas intensity in the region 1500–1800 cm^{-1} (sp^2 C=C stretch) has increased. This is also accompanied by an increase in sharpness and intensity of the peak at ~850 cm^{-1} (sp^2 C–H wagging in and out of the plane). Further, the apparent downwards shift in energy of the position of the main peaks is due to a considerable increase in intensity in the region ~950–1200 cm^{-1}, which is generally assigned to $-CH_2$ twisting and wagging vibrations. These changes are all consistent with the increase in the relative number of CH_2 groups observed in the analysis of the CH stretch region of the IR spectra, and the neutron diffraction data which show a higher sp^2 carbon content for this sample.

Finally, samples V and VI, prepared by PECVD, are similar to samples I and II, prepared by a FAB. The higher hydrogen content in the PECVD samples produces an increased relative intensity of the CH_2 and CH_3 deformation bands either side of the sp^3 stretch band at ~1250 cm^{-1}. The differences between the spectra for these two samples are small and on the whole result from the different hydrogen contents. The intensity in the sp^2 C=C

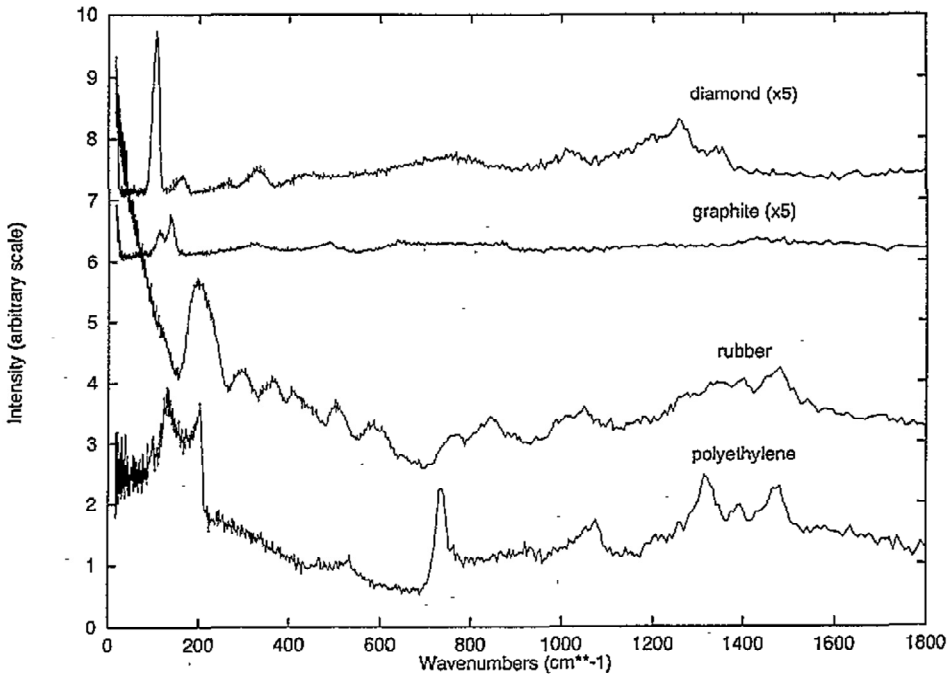

Figure 5. Raw INS data in the low-energy region for the 'standard' samples.

stretch region (above 1500 cm^{-1}) is about the same for the two samples, and is similar to that observed in samples I and II. The sp^2 CH in- and out-of-plane bends (~850 cm^{-1}) are also similar in all four samples. The low-energy regions (0–400 cm^{-1}) of the spectra for the PECVD samples show that there are some differences in network vibrations compared to those of the FAB-prepared samples; however, how these differences relate to changes in the network structure cannot be determined.

The diffuse reflectance IR data show similar trends among the a-C:H samples.

3.3. Summary

The results of the infrared and inelastic neutron scattering studies for these a-C:H samples are summarized below:

(i) in both the IR and INS data the modes are common to all samples, although with varying intensity;

(ii) from the INS results, the spectra for all a-C:H samples are *most* similar to those obtained for polymeric materials, rather than diamond and graphite, but with only short chains;

(iii) samples I and II prepared from acetylene and propane respectively, are very similar—this is evident from the neutron diffraction as well as the IR and INS results;

(iv) from neutron diffraction results, samples I and III (prepared at different deposition energies) have a very similar structure, but IR data show that the distribution of H within the network changes with deposition energy;

(v) sample IV, prepared from cyclohexane at ~960 V, is quite different from the other samples: it has relatively few CH_3 groups compared to the other samples and a much larger sp^2 carbon content—these differences are apparent from all the experimental results;

(*vi*) IR and INS data show that samples V and VI, prepared by PECVD, are similar to samples I and III (a conclusion which also emerged from the neutron diffraction results), although the increased H content gives increased intensity to CH_n deformation modes in the INS data.

4. Conclusions

Perhaps the most important point to emerge from these data is that for all the samples the results are consistent with a structural model for a-C:H derived from our previous work, which includes short, polymeric chains. Certainly the INS spectra for the a-C:H samples bear closest resemblance to the spectra obtained for the polymer materials, polyethylene and rubber, although the much lower scattering cross-section for carbon means that carbon–hydrogen correlations will dominate the spectra. The effects of varying some of the deposition parameters were also investigated and differences in the relative proportions of bonding environments were detected. It was found that, over the range of deposition conditions explored in this work, all the samples produced were very similar, except sample IV, which was produced from cyclohexane gas at high energy. This agrees with the neutron diffraction results [9, 20] which show only small differences in structure among the samples. However, the results for sample IV can be satisfactorily explained in terms of the subplantation model for deposition.

This work has also illustrated the value of infrared spectroscopy and inelastic neutron scattering as complementary experimental techniques.

Acknowledgments

We would like to thank M Weiler, S Sattel and T M Burke for preparing some of the samples, and A Fassam and G Bradley (Chemistry Department, UKC), respectively, for their help in the combustion analysis and infrared experiments. JKW acknowledges the receipt of an EPSRC studentship.

References

[1] Lettington A H 1991 *Diamond and Diamondlike Films and Coatings* ed J C Angus, R E Clausing, L L Horton and P Koidl (New York: Plenum) p 481
[2] Aisenberg S and Kimock F M 1989 *Mater. Sci. Forum* **52 + 53** 1
[3] Robertson J 1991 *Prog. Solid State Chem.* **21** 199
[4] Petrich M A 1989 *Mater. Sci. Forum* **52** 377
[5] Ehrhardt H, Kleber R, Kruger A, Dworschak W, Jung K, Muhling T, Engelke F and Metz M 1992 *Diamond Relat. Mater.* **1** 316
[6] Robertson J 1986 *Adv. Phys.* **35** 317
[7] Robertson J 1992 *Phys. Rev. Lett.* **68** 220
[8] Angus J C, Koidl P and Domitz S 1986 *Plasma Deposited Thin Films* ed J Mort and F Jansen (Boca Raton, FL: Chemical Rubber Company) ch 4, p 89
[9] Walters J K, Honeybone P J R, Huxley D W, Newport R J, and Howells W S 1994 *Phys. Rev.* B **50** 831
[10] Honeybone P J R, Walters J K, Newport R J, Howells W S and Tomkinson J 1994 *J. Non-Cryst. Solids* **169** 54
[11] Jäger C, Gottwald J, Spieß H W and Newport R J 1994 *Phys. Rev.* B **50** 846
[12] Jungnickel G, Frauenheim T, Blaudeck P, Stephan U and Newport R J 1994 *Phys. Rev.* B **50** 6709
[13] Walters J K and Newport R J 1995 *J. Phys.: Condens. Matter* **7** 1755
[14] Walters J K, Honeybone P J R, Huxley D W, Newport R J, and Howells W S 1993 *J. Phys.: Condens. Matter* **5** L387

[15] Walters J K, Fox D M, Burke T M, Weedon O D, Newport R J and Howells W S 1994 *J. Chem Phys.* **101** 4288
[16] Kleber R, Weiler M, A Krugler, Sattel S, Kunz G, Jung K and Ehrhardt H 1993 *Diamond Relat. Mater.* **2** 242
[17] Lifshitz Y, Kasi S R and Rabalais J W 1989 *Mater. Sci. Forum* **52 + 53** 237
[18] Veerasamy V S, Amaratunga G A J, Milne W I, Robertson J and Fallon P J 1993 *J. Non-Cryst. Solids* **164–166** 1111
[19] Lifshitz Y, Kasi S R and Rabalais J W 1989 *Phys. Rev. Lett.* **62** 1290
[20] Walters J K, Algar C D, Burke T M, Rigden J S, Newport R J, Bushnell-Wye G, Howells W S and Sattel S 1995 *J. Non-Cryst. Solids* at press
[21] Dischler B 1987 *Amorphous Hydrogenated Carbon Films* ed P Koidl and P Oelhafen (Paris: Les Editions de Physique) p 189
[22] Angus J C, Stultz J E, Shiller P J, MacDonald J R, Mirtich M J and Domitz S 1984 *Thin Solid Films* **118** 311
[23] Vandentrop G J, Kawasaki M, Kobayashi K and Somorjai G A 1991 *J. Vac. Sci. Technol.* A **9** 1157
[24] Walters J K, Rigden J S, Newport R J, Howells W S and Parker S F 1994 *Phys. Scr.* T **57** 142
[25] *User Guide to Experimental Facilities at ISIS* 1992
[26] Dworschak W, Kleber R, Fuchs A, Scheppat B, Keller G, Jung K and Ehrhardt H 1990 *Thin Solid Films* **189** 257
[27] Kleber R, Dworschak W, Gerber J, Kriigler A, Jung K, Ehrhardt H, Schulze S, Mühling I, Deutschmann S, Scharff W, Engelke F and Metz H 1991 *Mater. Sci. Eng.* A **140** 775
[28] Burke T M 1994 An X-ray and neutron scattering study of amorphous hydrogerlated carbon *PhD Thesis* University of Kent at Canterbury
[29] Axe J D 1976 *Physics of Structurally Disordered Materials* ed S S Mitra (New York: Plenum) p 507
[30] Tomkinson J 1988 *Neutron Scattering at a Pulsed Source* ed B D Rainford, R J Newport and R Cywinski (Bristol: Hilger) ch 12, p 324
[31] Honeybone P J R, Newport R J, Howells W S, Bennington S M and Revell P J 1991 *Physica* B **180 + 181** 787
[32] Honeybone P J R, Newport R J, Walters J K, Howells W S and Tomkinson J 1994 *Phys. Rev.* B **50** 839
[33] Lukins P B, McKenzie D R, Vassallo A M and Hanna J V 1993 *Carbon* **31** 569
[34] Dischler B, Bubenzer A and Koidl P 1983 *Solid State Commun.* **48** 105
[35] González-Hernandez J, Chao B S and Pawlik D A 1989 *Mater. Sci. Forum* **52 + 53** 543
[36] Parker S F 1994 *Appl. Spectrosc.* **48** 669
[37] Dehbi-Alaoui A, Matthews A and Franks J 1991 *Surf. Coatings Technol.* **47** 722
[38] Field J E 1979 *Properties of Diamond* (New York: Academic)
[39] Kelly B T 1981 *Physics of Graphite* (London: Applied Science)
[40] Ashby M F and Jones D R H 1980 *Engineering Materials* (Oxford: Pergamon)